Programmed Electrochemical Exfoliation of Graphite to High Quality Graphene

Duhong Chen,[a] Fei Wang,[a] Yijuan Li,[a] Weiwei Wang,[a] Teng-Xiang Huang,[a] Jian-Feng Li,[*,a] Kostya S. Novoselov,[a, b] Zhong-Qun Tian[a] and Dongping Zhan[*, a]

[a] *State Key Laboratory of Physical Chemistry of Solid Surfaces, Collaborative Innovation Center of Chemistry for Energy Materials, Engineering Reseach Center of Electrochemical Technologies of Ministry of Education, Department of Chemistry, College of Chemistry and Chemical Engineering, and Graphene Industry and Engineering Research Institute, Xiamen University, Xiamen 361005, China.*

[b] *School of Physics and Astronomy, University of Manchester, Oxford Road, M13 9PL Manchester, UK.*

S1 Chemicals and materials

Highly ordered pyrolytic graphite (HOPG, 10 mm × 10 mm × 1 mm) and polypropylene filter membrane (pore size: 200 nm) were provided by shanghai NTI Co., Ltd.. The commercial 5-mm-diamtert graphite rods was purchased from Qingdao Dadi Carbon technology Co., Ltd.. Sulfuric acid (H_2SO_4), sodium sulfate (Na_2SO_4), ammonium sulfate ($(NH_4)_2SO_4$) and N, N-dimethyl formamide (DMF) were analytical grade provided by Sinopharm Co., China. All aqueous solutions were prepared with deionized water (18.2 MΩ•cm, Milli-Q, Millipore Co.).

S2 Measurements and instruments

All the electrochemical experiments were carried out with a CHI 631B electrochemical workstation (CHI Co., USA) or a high-power MD-30 electrochemical workstation (Xiamen Qunji Instrument Co., China). Field emission scanning electron microscope (FESEM: LEO 1530 Gemini, Zeiss Co., Germany), transmission electron microscope (TEM: JEM-2100, JEOL Co., Japan), atomic force microscopy (AFM, NTEGRA, NT-

MDT, Moscow, Russia), confocal laser microscope (XploRA, Horiba Jobin Yvon Co., Japan), X-ray diffraction (XRD, Rigaku Ultima IV X, Japan), Brunauer-Emmett-Teller (BET, Micromeritics Tristar II 3020 analyzer, USA), X-ray photoelectron spectroscopy (Quantum 2000 XPS, PHI Co., USA) were employed to characterize the graphene obtained by electrochemical exfoliation.

S3 Cyclic voltammetry of the basal face of HOPG

In this experiment, we sealed HOPG plate with an exposed disc area (diameter: 3 mm) of the basal face. Cyclic voltammetry was performed as shown in Fig. S1. It is observed that a small current wave at an onset potential of 1.45 V followed by a second wave 1.75 V. If the reverse potential is set at 1.75 V, the exposed HOPG area will expand and becomes very rough after a few cycles. After 1.75 V, oxygen evolution reaction (OER) will occur coupling with the oxidation of carbon, i.e., the break of carbon-carbon bond and the formation of various carbon-oxygen bond which is defined as the surface tailoring in the text. From the CV we can deduce that the kinetic rate of ion intercalation is much slower than that of the OER. Knowing this, we can seek a balance between the ion intercalation and the OER as well as the surface tailoring processes. The surface tailoring processes were recorded as in Fig. 2 by in-situ electrochemical AFM imaging experiments.

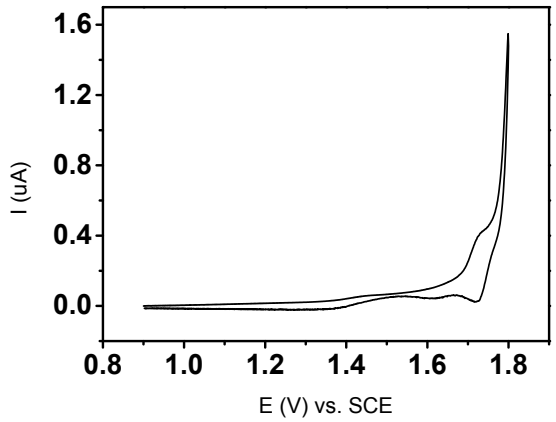

Fig. S1 Cyclic voltammogram of HOPG electrode in 2 M $(NH_4)_2SO_4$, scan rate: 10 $mV \cdot s^{-1}$.

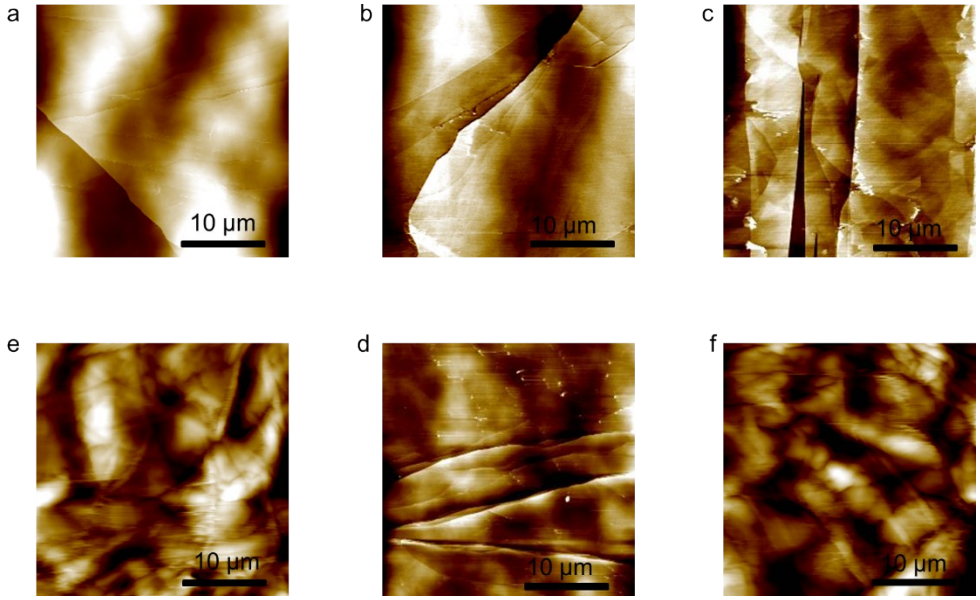

Fig. S2 (a-f) are the EC-AFM images of the HOPG basal faces at 5, 6, 7, 8, 9 and 10 V, indicating that the higher the applied potential, the fast the surface tailoring.

S4 Programmed electrolysis of graphite

The programmed electrolysis of graphite is conducted in 0.1 M $(NH_4)_2SO_4$ solution and Pt foil used as counter electrode. Programmed potential modulations used in our experiments are listed as in Fig. S3a. At first, we design the simple potential pulses by electrolyzing the graphite at different anodic potentials for 1 second and relaxing the electrolysis processes at -0.5 V for 3 seconds, which forms one electrolytic period. We optimized the potential region as [7.0 V, 10.0 V] based on the considerations of both the electrolytic efficient and the quality of the product Gr. Then, different potential modulations were tried and found that the sinusoidal protocols was the best. The relaxing process at -0.5 V is really a good idea because the surface tailoring and bubbling dispersion were ceased, and the intercalated ions were de-intercalation and thus released. The repeated intercalation and de-intercalation was demonstrated very useful to improve the size and to decrease the layer numbers. Furthermore, the intermittent surface tailoring was helpful to decrease the oxidation degree of the produced Gr.

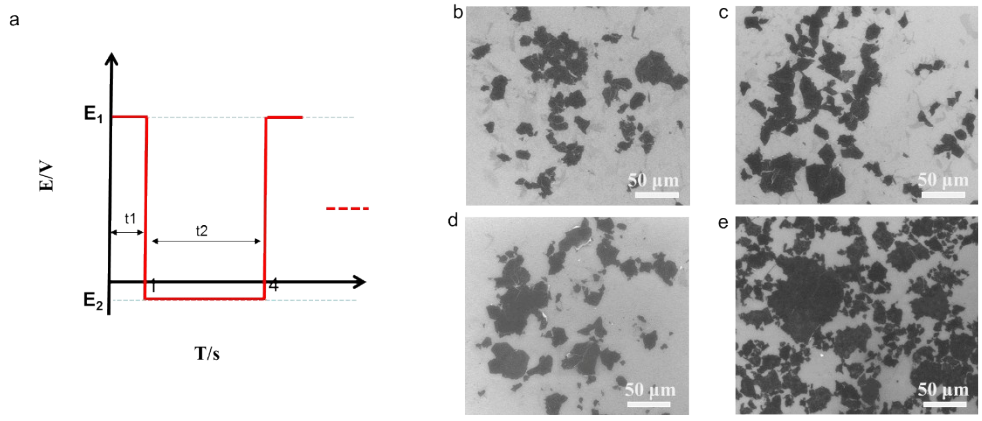

Fig. S3 (a) The square-wave potential protocols for electroexfoliation of HOPG, (b-e) the SEM images of Gr obtained at exfoliation potential of 7.0, 8.0, 9.0 and 10.0 V.

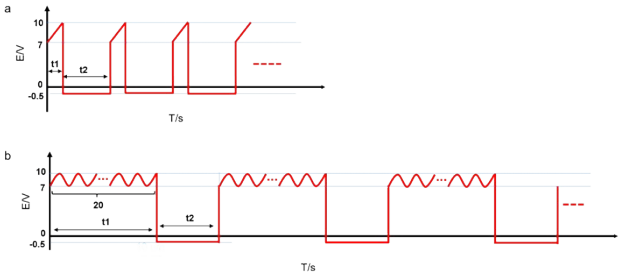

Fig. S4 (a) The linear potential protocol and (b) the sinusoidal protocol for the electrochemical exfoliation of HOPG respectivity.

S5 Measurements of AFM, SEM, TEM, XRD, XPS and BET

As described in the text, the oxidation degree of the electrolytic Gr is pretty low. Thus, the solubility of the obtained Gr in aqueous solution is low. The aqueous suspension of Gr was filtered by using a poly(tetrafluoroethylene) (PTFE) filter membrane with an average pore size of 200 nm. The filtered Gr was then dispersed in water by ultrasonic and filtered for several times to remove the residual $(NH_4)_2SO_4$. The clean Gr was dispersed ultrasonically in DMF in ice-water bath for 15 minutes and a dispersion of ~2.5 mg/mL was obtained. After reserved for two days, little precipitations were found in the bottom of the glass bottle. That means the yield of the Gr with fewer layers were pretty high. The Gr was diluted further and dropped on a 300-nm-thickness SiO_2 covered Si wafer for SEM, AFM, normal Raman and the Raman mapping experiments, or dropped on the Cu mesh for TEM experiments. And

the Gr/DMF suspension was filtered and dried for the XRD, BET and XPS experiment.

From the high-resolution TEM (HRTEM) images we can observe the edge area of the Gr with different layers. However, this statistics by HRTEM is time comsuming. We used AFM to measure the layers of Gr and calculated the layer distributions. The 1-4 layers of Gr obtained from the programed electrolysis of commercial graphite rod was shown in Fig. S5. The BET results show that the specific area of 230.2 m^2 g^{-1} (Fig. S7). XRD data of the graphene obtained by the commercial available graphite rod was shown in Fig. S8. According to the Bragg's Law ($2d\sin\theta = n\lambda$), the lower the θ is, the bigger the interlayer distance would be. The broad peak of graphene showed a very non-uniform interlayer distance which is actually caused by the layer numbers of graphene themselves as well as the stack of graphene in the assembly process. The XRD spectrum is very similar to the phase structure of reduced oxidative graphene (rGO),[1-3] indicating that the low oxidation degree of our graphene.

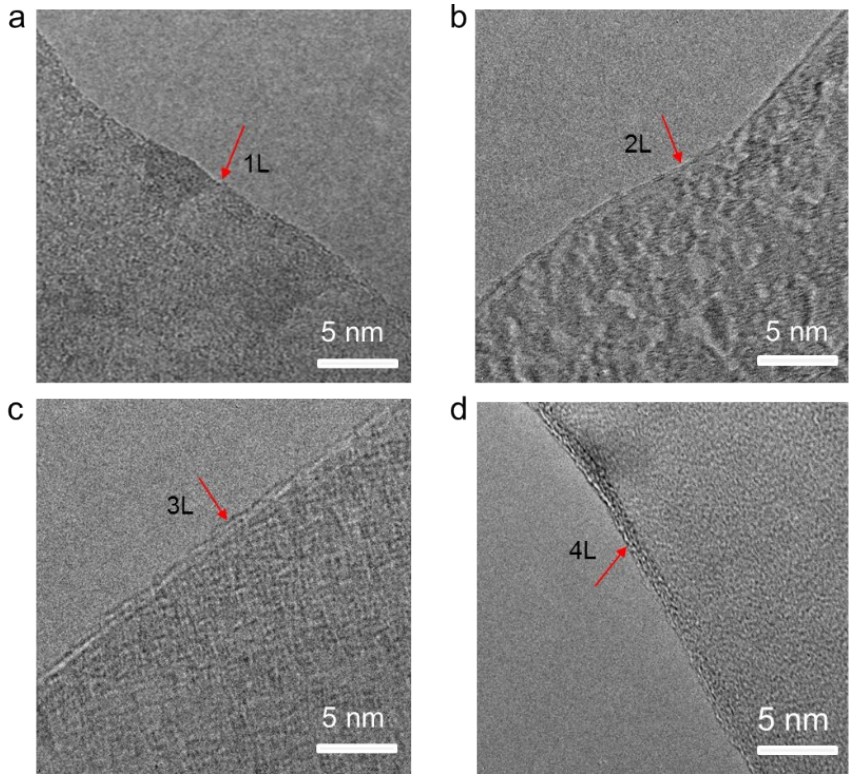

Fig. S5 The TEM images of 1-4 layers of Gr obtained by electrochemical exfoliation of graphite rod.

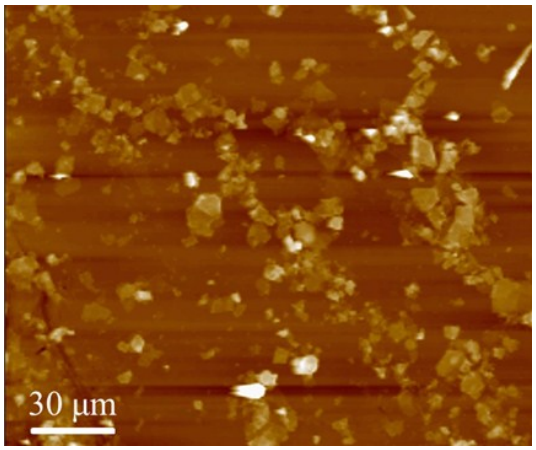

Fig. S6 The AFM images of Gr obtained by electrochemical exfoliation of graphite rod.

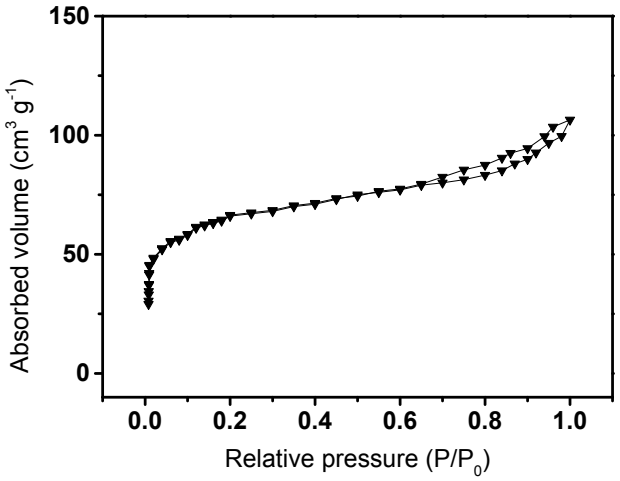

Fig. S7 BET images of Gr obtained by electrochemical exfoliation of graphite rod.

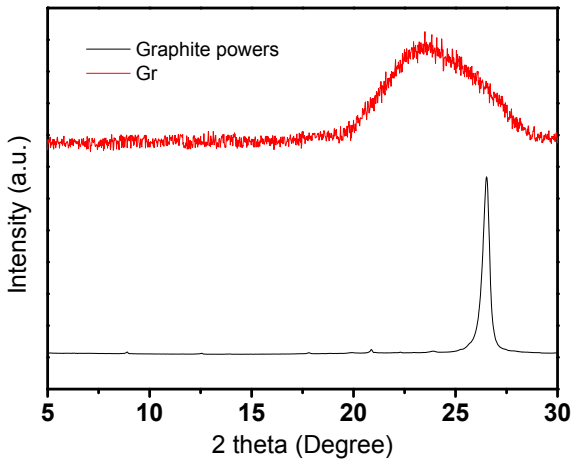

Fig. S8 The XRD images of Gr and graphite powers.

S6 The calculation method for the yield of Gr

(1) Measuring the mass of the raw material (HOPG or the commercial graphite rod) before experiment and marking it as M1.

(2) Measuring the mass of the filtered Gr from the DMF suspension after discarding the precipitations therein and marking it as M2.

(3) Calculating the yield of Gr by the equation: Yield % = (M2/M1)×100%

S7 The fabrication and characterization protocols of the Gr supercapacitor

Two Gr papers are prepared by filtering the Gr /DMF suspension with the PTFE filter membrane. The total mass of the two Gr paper were measured and marked as *m*. A polypropylene film was adopted as the separator and an aqueous solution with 1 M Na_2SO_4 was adopted as the electrolyte of the supercapacitor. Two stainless steel plates (diameter: 2 cm) were adopted as the current collector. All these are assemblied and sealed as a button cell for the cyclic voltammetry and charging/discharging experiments. The specific capacity of the demo-device was calculated by the following equation:

$$C = I/m \times (\frac{\Delta t}{\Delta V}) \quad (1)$$

Where C (F g^{-1}) is the measured capacitance, I (A) is the constant discharging current, Δt/ΔV represents the reciprocal of the slope of the discharge curve, m (g) is the mass of the Gr paper. The electrochemical impedence spectroscopy (EIS) experiment were performed amd the inner resistance and the charge transfer resistance were obtained as 2.0 Ω and 0.75 Ω, indicating a good conductance of the graphene and a compact assembly of the supercapacitor

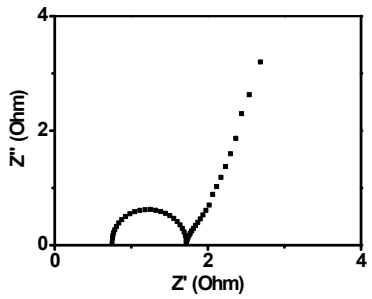

Fig. S9. The EIS spectrum of Gr-based supercapacitor.

Table S1 The comparison of various methods used to electrolysis of Graphite rod

Methods	The average areas of Gr (μm^2)	References
Sinusoidal potential waves	50	This work
Constant current	<10	Ref. 4
Constant voltage	<2	Ref. 5
Constant voltage	<8	Ref. 6
Constant voltage	<1	Ref. 7
Constant voltage	NM	Ref. 8
Constant voltage	NM	Ref. 9

References

[1] S. Park, J. An, J. R. Potts, A. Velamakanni, S. Murali and R. S. Ruoff, *Carbon*, 2011, **49**, 3019.

[2] K. Krishnamoorthy, M. Veerapandian, K. Yun and S. J. Kim, *Carbon*, 2013, **53**, 38.

[3] L. Stobinski, B. Lesiak, A. Malolepszy, M. Mazurkiewicz, B. Mierzwa, J. Zemek, P. Jiricek and I. Bieloshapka, *J. Electron Spectrosc*, 2014, **195**, 145.

[4] Liu, J.; Poh, C. K.; Zhan, D.; Lai, L.; Lim, S. H.; Wang, L.; Liu, X.; Gopal Sahoo, N.; Li, C.; Shen, Z.; Lin, J. *Nano Energy* **2013**, *2*, 377.

[5] Coros, M.; Pogacean, F.; Rosu, M.-C.; Socaci, C.; Borodi, G.; Magerusan, L.; Biris, A. R.; Pruneanu, S. *RSC Adv.* **2016**, *6*, 2651.

[6] Hamra, A. A. B.; Lim, H. N.; Chee, W. K.; Huang, N. M. *Appl. Surf. Sci.* **2016**, *360*, 213.

[7] Gorle, D. B.; Kulandainathan, M. A. *J. Mater. Chem. A* **2017**, *5*, 15273.

[8] Yang, F.; He, D.; Zheng, B.; Xiao, D.; Wu, L.; Guo, Y. *J. Electroanal. Chem.* **2016**, *767*, 100.

[9] Cooper, A. J.; Wilson, N. R.; Kinloch, I. A.; Dryfe, R. A. W. *Carbon* **2014**, *66*, 340.